Automatika

Journal for Control, Measurement, Electronics, Computing and Communications

ISSN: 0005-1144 (Print) 1848-3380 (Online) Journal homepage: https://www.tandfonline.com/loi/taut20

# 3D sensing of back symmetry curve suited for dynamic analysis of spinal deformities

Matea Đonlić, Tomislav Petković, Stanislav Peharec & Tomislav Pribanić

**To cite this article:** Matea Đonlić, Tomislav Petković, Stanislav Peharec & Tomislav Pribanić (2018) 3D sensing of back symmetry curve suited for dynamic analysis of spinal deformities, Automatika, 59:2, 172-183, DOI: 10.1080/00051144.2018.1517513

**To link to this article:** https://doi.org/10.1080/00051144.2018.1517513

AUTOMATIKA
2018, VOL. 59, NO. 2, 172–183
https://doi.org/10.1080/00051144.2018.1517513

REGULAR PAPER

OPEN ACCESS Check for updates

# 3D sensing of back symmetry curve suited for dynamic analysis of spinal deformities

Matea Đonlić [a], Tomislav Petković [a], Stanislav Peharec[b] and Tomislav Pribanić[a]

[a]Faculty of Electrical Engineering and Computing, University of Zagreb, Zagreb, Croatia; [b]Polyclinic for Physical Medicine and Rehabilitation Peharec, Pula, Croatia

**ABSTRACT**

This paper is focused on meeting the demands for better detection and evaluation of the spinal deformities that go beyond a basic static 3D analysis. It is expected that by observing the spine while it moves an improved 3D deformity analysis and measurements can be achieved. In this paper, we present a novel approach for the automatic back symmetry curve sensing. Our approach can be used in the back shape analysis of many different positions, i.e. segments of the dynamic motion, and is not limited only to the upright standing position. The proposed method is based on the 3D surface reconstruction, surface curvature analysis and graph theoretic approach for the (semi-)automatic detection of the symmetry curve. In addition, we introduce a 3D scanning system which was used in our experiment to successfully generate 3D back surface reconstructions for each frame of the captured forward bending motion. We also tested the proposed method on the data collected using commercial 3D spine analysis system and the results were comparable. The additional experiment focusing on the dynamic analysis demonstrated that the proposed method can enable further advances in the automatic 3D back surface analysis by tracking the spine position throughout performed movements.

**ARTICLE HISTORY**
Received 24 April 2018
Accepted 27 August 2018

**KEYWORDS**
3D Back shape analysis; stereophotogrammetry; spinal deformities; surface curvature analysis; symmetry curve; forward bending motion

## 1. Introduction

Spinal deformities are a growing problem in today's society due to the current sedentary lifestyle. Scoliosis, defined as lateral curvature of the spine, is one of the most common spinal deformities. Based on the US statistics [1], scoliosis affects two to three percent of the population, usually kids in their early teens and adolescents [2], but adults can also suffer from either idiopathic or degenerative scoliosis [3]. The practice shows that the early detection of all spinal deformities is an important factor in the prevention of progression and the deformity correction. Consequently, general physical examinations which include screening for the scoliosis indications are conducted for the children in the primary school. Screening is usually performed by an experienced physician, using a visual examination and a forward bending test (Adam's test [4]) combined with the scoliometer. In Croatia during the primary school education, spine examination is carried out usually in the fifth and the eighth grade [5]. According to the National Scoliosis Foundation [6], screenings in the USA are not uniformly regulated and can vary from only one screening to more then four screenings (rarely). Children with diagnosed signs of the deformity are in general referred to a hospital where radiographs are taken. These radiographs are usually 2D assessments which do not take the full 3D deformity into account, although there are some examples of using biplanar radiographs to compute the 3D shape of the spine [7]. Most importantly, regular radiographs have negative effects on health so radiography should be used only when highly necessary and not as a preventive regular examination procedure.

Due to a large number of patients and a limited number of physicians, preventive examinations cannot be done frequently and in more detail. Therefore, there is a need for the use of new approaches to the detection of spinal deformities and treatment monitoring. A non-invasive approach to body analysis, which is much more accessible today, is the use of an optical 3D surface scanning system that enables faster and more detailed examinations. Systems for the 3D body surface reconstruction and its analysis are extremely useful for the diagnostics of spinal deformity, since they can provide repeatability of measurements (reducing the influence of physician's variability) and allow an objective comparison of two measurements performed in a certain time interval, e.g. when monitoring progression or treatment success. Optical surface scanning systems cannot directly reconstruct the 3D spine shape and therefore the 3D analysis is focused on the back shape morphology. Spinous processes are rarely visible on the surface of the back due to the skin and tissue that covers them and their detection can be achieved using

**CONTACT** Matea Đonlić matea.donlic@fer.hr Faculty of Electrical Engineering and Computing, University of Zagreb, Unska 3, HR-10000 Zagreb, Croatia

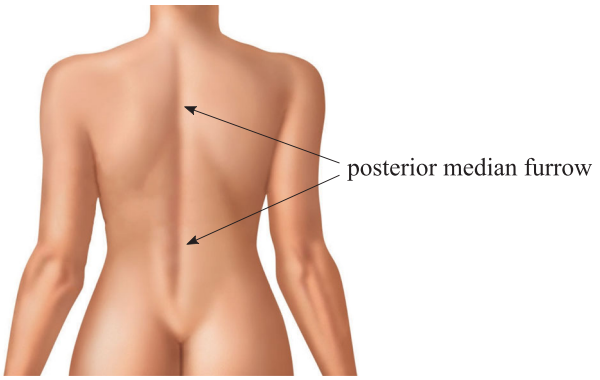


**Figure 1.** An illustration of the posterior median furrow present on the human back.

*direct methods* by placing adhesive markers on spinous processes, typically 6–12 markers in total [8–10]. Alternatively, *indirect methods* are based on the approximation of the curve that connects spinous processes along the entire spinal column which is associated with the posterior median furrow[1] (Figure 1). The usual indirect methods are based on the back surface curvature analysis and the approximation of the posterior median furrow with the maximal surface curvature, and on the analysis of the back surface symmetry and finding the maximum symmetry curve or the minimum asymmetry curve [12].

The proposed idea for our back symmetry analysis is motivated by Hierholzer [13] who suggests that analysis of the surface curvature is the optimal choice because the curvature has a nice property of being invariant to the surface rotation and translation. Furthermore, even though the surface curvature alone can be used to estimate spinal deformities, the left–right differences of the surface curvature distribution (the asymmetry function) are a better descriptor for the deformities which are present across the entire back surface.

In this paper, we first give a short introduction to the 3D surface scanning procedures followed by an overview of different approaches to the back surface analysis. Next, we explain how we propose to collect back surface data using our affordable 3D scanning system. Along with the proposed approach to 3D scanning in dynamics, we present a method which can detect a symmetry curve of the back and surpass the analysis of the back in the pure upright standing position. Finally, we present our experiments in the "Results and discussion" section which is followed by a short conclusion.

## 2. Related work

Considering 3D body surface scanning, state-of-the-art approaches for optical 3D shape measurement include laser scanning [14], structured light (SL) profilometry [9] (including digital rasterstereography [15]) and stereophotogrammetry [16]. All above-mentioned approaches produce a high-quality surface representation but they differ in pricing, system limitations, acquisition time and postprocessing requisitions. For example, laser scanning produces the top quality scans at the cost of longer acquisition times and higher expenses. SL profilometry and stereophotogrammetry are approaches which can produce a dense 3D surface reconstruction using a simple set-up and low-cost components (cameras and projectors). Compared with SL profilometry, the stereophotogrammetry has less limitations considering the freedom in the positioning of system components (cameras/projectors) while retaining the low acquisition time and the 3D surface reconstruction of moving objects.

The early work of spinal analyses, which is focused on analyses of the 3D back surface using indirect methods, was conducted by Frobin, Hierholzer and Drerup at the University of Münster in Germany in 1980s. For the acquisition of the three-dimensional surface of the back they used rasterstereography [17]. Frobin and Hierholzer [18] showed that the analysis of the back surface curvature is very useful for the study of scoliosis thanks to the geometric properties of the curvature that enable a reliable detection of asymmetries independent of the patient's position with regard to the acquisition system. That is an important property because due to the torsion, parts of the back can be differently oriented to the scanning system, which should not impact the correct analysis.

Hierholzer [13] was the first to propose a new method for the detection of the minimum asymmetry line of the back. His procedure is based on the analysis of the distribution of the back surface curvatures and the definition of the (lateral) asymmetry function. The reconstructed 3D back surface is sectioned with horizontal planes in a number of slices, resulting in a single curve of the back profile for each slice. Each profile curve is evaluated using the asymmetry function and the point with the minimum value is chosen as the symmetry point of the observed profile. Since there is a possibility of multiple relative minima of the asymmetry function, Drerup and Hierholzer [19,20] proposed a new method that uses a mathematical spinal model which out of all possible candidates (relative minima) in each profile chooses those points that are the best fit to the chosen spinal model over the whole back. These studies were initially developed for the Formetric Project [15,21] which was commercialized in the '90s and is now actively used for scoliosis diagnosis in the upright standing position.

Poredoš et al. [14] use laser scanning of the back to generate the 3D depth map of the back. Using depth image, they calculate the surface curvature along the horizontal direction, for each row of the image individually. The detection of the posterior median furrow curve is done using the detection of the extreme values of the calculated surface curvature. This method results

in the detection of multiple spurious extrema and user-intervention is required for choosing the curve which best describes the furrow line of the back.

Di Angelo et al. [22] base their method on the work of Hierholzer [13], i.e. the detection of the back symmetry line. Instead of using the distribution of the back surface curvatures for defining the asymmetry function, they propose to use calculated surface normals. Additionally, they use the spine model based on the 75 healthy subjects [23] for the selection of the best relative minima between all possible candidates obtained with the evaluation of the asymmetry function on each horizontal slice of the back surface. They extend the method by proposing the Frenet-Serret frame [24] for defining local coordinate systems, improving the curve detection, and achieving the detection of a minimal asymmetry line even in the asymmetric postures of subjects [25].

Huysmans et al. [26] use active shape models (ASM) for the 3D reconstruction of the spinal shape. A set of x-rays of 264 scoliotic patients was used as a labelled training set for the statistical analysis of vertebral body centres locations in 3D, i.e. scoliotic curve patterns. The derived point distribution model (PDM) gives expected positions of the vertebral centres and has a set of parameters which control modes of variation present in the training set. The ASM is a "smart snake" model [27] which is able to iteratively deform in a way characteristic for an object described with the training set. To initialize the ASM from the mean shape of the PDM, the previously detected locations of vertebrae C7 and vertebrae L4 are used. Then, a set of adjustments that iteratively leads to the minimal solution is found, where the objective is to minimize the total asymmetry of the ASM.

Bergeron et al. [28] propose a learning-based approach to achieve a robust relation between the scanned trunk surface and the spinal data from x-rays. Authors propose using functional data analysis and train multiple support vector regression (SVR) machines to predict spinal curve coefficients from the functional coefficients of the trunk surface derived using functional principal component analysis . This approach shows a robust predictive capability but with some poor SVR prediction in few cases which needs to be solved before any implementation for the clinical setting.

## 3. Materials and methods

Three-dimensional back surface data were collected using two different 3D scanners – a commercial 3D Diers Formetric system and a proposed self-made low-cost 3D body scanner. Scanners differ in configurations and scanning capabilities: the former can be used to scan subjects only in upright standing positions and the latter can be used to scan subjects in both standing and forward bend positions. The proposed method for the back surface analysis can be applied on the 3D back surface data collected using both scanners. The 3D analysis is used to detect the symmetry curve of the back based on the analysis of surface curvature asymmetries.

### 3.1. Diers Formetric 3D system

The Diers Formetric system is a commercial device for rasterstereographic surface reconstruction with back surface analysis [15,21]. A set of thin horizontal stripes are projected onto subject's back and, using the image captured with a camera, reconstructed as a 3D profile section curves as depicted in Figure 2. The recording frequency is 10 FPS and a total acquisition recording sequence can go up to 60 seconds depending on whether the averaging between scans is used. The system is composed of an operating unit, a lifting column, a stripe projector and a camera which occupy a space

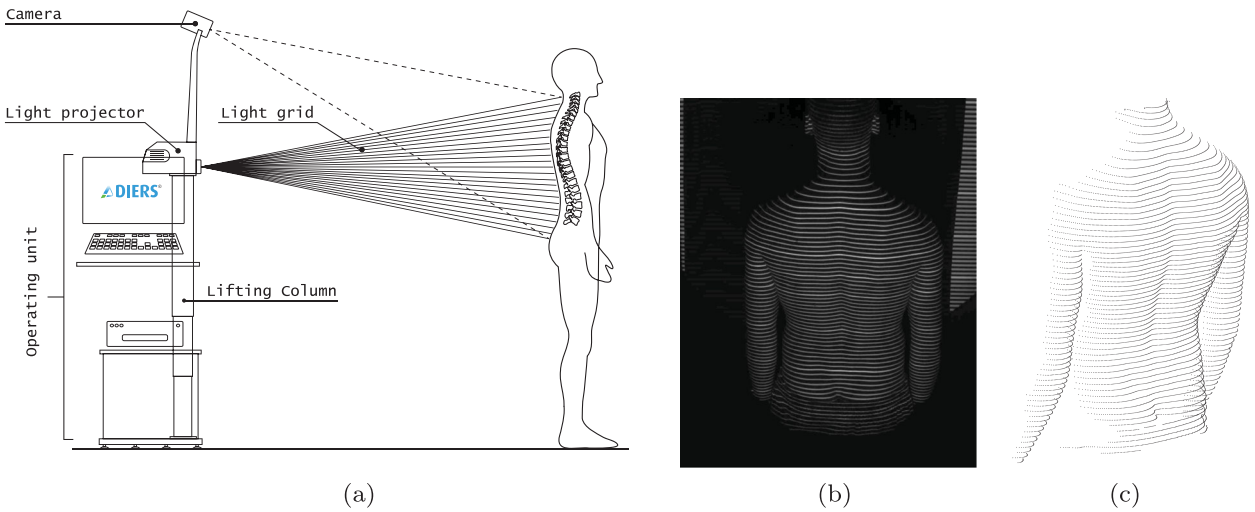


**Figure 2.** An example of data collected using the Diers Formetric system for one specific patient. (a) The Diers Formetric system [21]. Reproduced from online published catalogue [29]. (b) Image captured by system's camera. (c) Back surface 3D reconstruction.

of approximately 3 × 1.5 × 2.5 metres including the required distance from the scanned subject. The basic equipment of the system also includes a black velvet backdrop which is advised to place in front of the subject in order to reduce reflections and to enhance the subject-background contrast.

The Diers Formetric analysis includes the detection of anatomical landmarks, computer-generated 3D spine model based on the surface curvature estimation and back surface reconstruction. Also, the final report includes various measures and clinical parameters which aid physicians in the diagnostic process.

#### 3.1.1. 3D scanning procedure – upright standing position

The Diers Formetric system is limited to the analysis of the patient's back surface only in the upright standing (or sitting) position. A subject is positioned in front of the 3D scanner at a specific distance range, exposing his/hers back to the system. The height of the scanning system is adjusted so the projected stripes illuminate the entire surface of the back. The subject is asked to stand still in a relaxed position and the scanning is done in few seconds.

### 3.2. Proposed 3D scanner

Based on the application of the 3D scanner for back analyses, a method of choice for 3D scanning was stereophotogrammetry, a stereo surface reconstruction approach, augmented with an additional texture projection.

A stereophotogrammetry requires at least two cameras which simultaneously capture an image of a scanned object. If one matches the position of an object's point in the image captured by the first camera with its position in the image captured by the second camera using a stereo-matching algorithm [30], the 3D coordinates of the point are determined using the triangulation. Scanning a smooth, flat, uni-coloured objects such as human back, requires the use of an active lighting device, e.g. a projector which projects a texture on the object. A projected texture enables easier matching of the corresponding points in captured images, and thus obtaining a dense 3D surface reconstruction. This stereophotogrammetry approach with a projected texture is a flexible 3D scanning solution where system components have only a few limitations on their positioning, i.e. the common field of view between cameras–projector pair. The number of employed scanning units is unconstrained provided that the overlapping projected texture remains distinctive enough to successfully apply a chosen stereo-matching algorithm.

Our 3D acquisition system is composed of two scanning units, placed one opposite to the other, both facing the subject that is being scanned. The system occupies a space of around 3.5 × 1 × 2.5 metres. Each unit is composed of one DLP projector and two cameras (Figure 3(a)). With this configuration we can successfully capture a 3D back surface of the subject, both in standing position and while bending forward. We used DLP projectors Acer S1383Whne paired with two PointGrey's Grasshopper3 GS3-U3-23S6C cameras with Fujinon HF12.5SA-1 lenses each. For the projected texture pattern, we adapted the speckle pattern proposed by Zhang et al. [31] and generated a pattern using two-dimensional discrete Fourier Transform (Figure 3(b)). With this configuration we are able to acquire data with 30 FPS on average. By employing a precise synchronization between cameras [32,33] we are able to obtain a 3D surface reconstruction of subject's front and back for each frame acquired during the scanning procedure.

Reconstructed 3D surfaces were denoized and smoothed as a part of a processing step of the reconstruction. We calibrated two scanning units wrt the

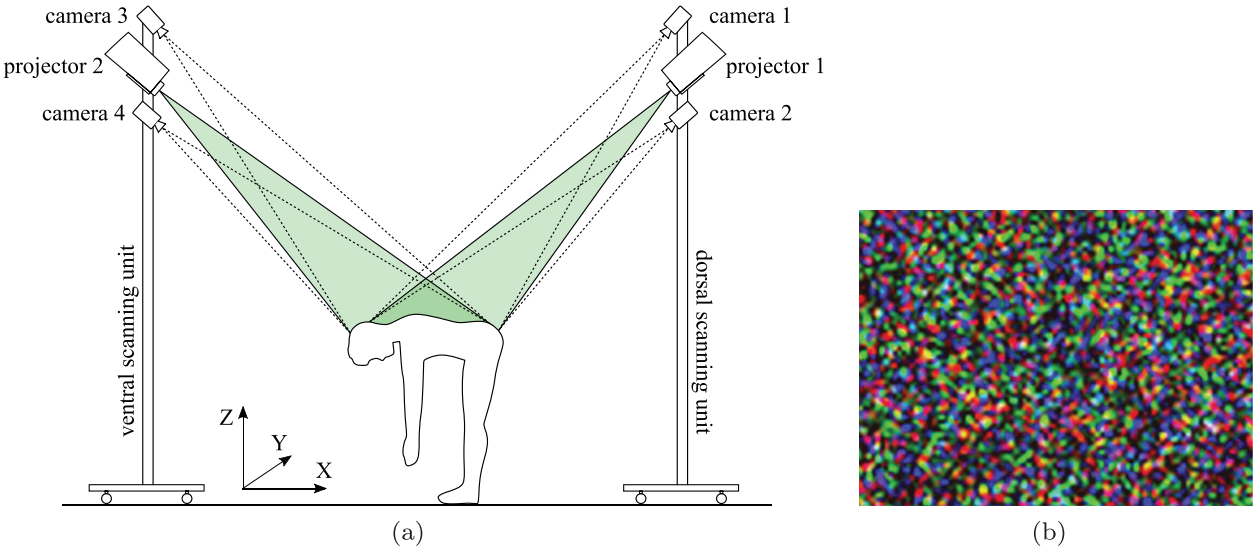


**Figure 3.** Proposed 3D scanning system. (a) Scanning system set-up. (b) Projected texture.

common coordinate system (a similar approach as presented in [33]) so the two point clouds can later be registered. The coordinate system of the 3D scanner is calibrated such that $XY$ plane is parallel with the floor and the $X$ axis connects the two scanning units.

#### 3.2.1. 3D scanning procedure – forward bending motion

For the dynamic scanning of a subject during forward bending motion, we propose the following procedure. A subject is placed halfway between the two scanning units, approximately 1.5 m from each unit, so one unit provides ventral and another dorsal view of the subject. At the beginning of the scanning, the subject is standing in an upright position, and then starts a forward bending motion until reaching a borderline comfortable position. The bending procedure is not limited in its duration but the total acquisition time is approximately five to seven seconds.

Due to the fact that each scanning unit acts as a separate scanning device and produces one point cloud each, it was necessary to merge those two point clouds into one final 3D surface of the back. Let us denote the point cloud reconstructed from the acquired frame $f_i$ using the dorsal scanning unit with $pc_1$ and the point cloud reconstructed using ventral scanning unit with $pc_2$. We start by using only the point cloud $pc_1$ reconstructed from the first frame $f_1$ as our *merged* point cloud. Then, for each following frame $f_i, i > 1$, we merge the point cloud $pc_1$ with the portion of the point cloud $pc_2$ that falls inside the predefined bounding box that surrounds the *merged* point cloud from the frame $f_{i-1}$. With this approach, we successfully keep only the point cloud representing the back surface and eliminate the portion of the point cloud representing the front of the scanned subject. The merged point cloud is then smoothed in order to eliminate small discrepancies due to potential inter-unit calibration error. The surface normals for each point are estimated as a preparation for the further back surface analysis.

### 3.3. Back surface analysis

Hierholzer [13] defined a surface asymmetry function of a point on a surface profile as the sum of local deviations of surface curvature across some predefined neighbourhood (profile region). Let $p$ be a point on the chosen surface profile $\Gamma : t \to (x, y, z)$. The asymmetry function $A(p)$ over the symmetrical profile region $\Lambda$ of length $L$ centred at the point $p$ is defined as

$$A(p) = \frac{1}{L}\int_{\Lambda}\left(\frac{1}{\pi}\int_{0}^{\pi}\left(\kappa_l(\alpha) - \kappa_r(\alpha)\right)^2 \mathrm{d}\alpha\right)\mathrm{d}t, \quad (1)$$

where $\kappa_l(\alpha)$ and $\kappa_r(\alpha)$ are normal curvatures [34] of symmetrical left and right neighbours of the point $p$ on the profile and where the dependence on the parameter $t$ is omitted for clarity. A normal curvature $\kappa(\alpha)$ can be computed for each direction $\alpha \in [0, \pi\rangle$ in the tangent plane of a surface point. The principal curvatures $\kappa_1$ and $\kappa_2$ are the minimum and the maximum values of the normal curvature. Using the differential geometry of 3D surfaces [13,34] the inner integral in Equation (1) can be explicitly computed using the estimations of the principal curvatures and principal directions for each point in the region $\Lambda$. The explicit solution is:

$$A(p) = \frac{1}{L}\int_{\Lambda}\Big((H_l - H_r)^2 + (G_l^2 - 2G_lG_r\cos(2\epsilon) + G_r^2)/2\Big)\,\mathrm{d}t, \quad (2)$$

where $H = (\kappa_1 + \kappa_2)/2$, $G = (\kappa_1 - \kappa_2)/2$, and $\epsilon$ is the difference angle between corresponding left–right principal directions (directions in the normal plane where the curvature takes its maximum and minimum).

If the surface is represented by a twice differentiable continuous function, the principal curvatures $\kappa_1$ and $\kappa_2$ can be determined as the eigenvalues of the associated Hessian matrix, while the eigenvectors are corresponding principal curvature directions. In practice, the surface is not a continuous function, but the elements of the Hessian matrix can be estimated from the point cloud and the associated surface normals using a first-order Taylor expansion and a least-squares method [35].

One practical problem of the asymmetry function $A(p)$ is that it produces a large number of minima which needs to be efficiently filtered in order to automatically detect the symmetry curve of the patient's back.

#### 3.3.1. Detection of the 3D symmetry curve

We adopted Hierholzer's definition (Equation (1)), which means that the goal is to find points with minimal asymmetry that represent the symmetry curve of the back.

For each transversal slice of the 3D back surface, we compute the asymmetry function in every point interpolated over the surface profile with 1 mm sampling distance using trapezoidal numerical integration. We densely slice 3D back surface using transversal planes (one slice every 5 mm) and create a two-dimensional asymmetry map of the back, where rows represent transversal slices and columns represent sampled points in the slice. The asymmetry map is represented as a 2D array to simplify the implementation and further calculations. A valid theoretical assumption is that asymmetry function will achieve minimal values at points which are on the symmetry curve that coincide with the posterior median furrow. However, it is possible that for a specific profile some relative minima may be a better choice than the absolute minima. For example, when a point on the prominent scapula is the absolute minima and a point on a posterior median furrow is a relative minima as depicted in Figure 4.

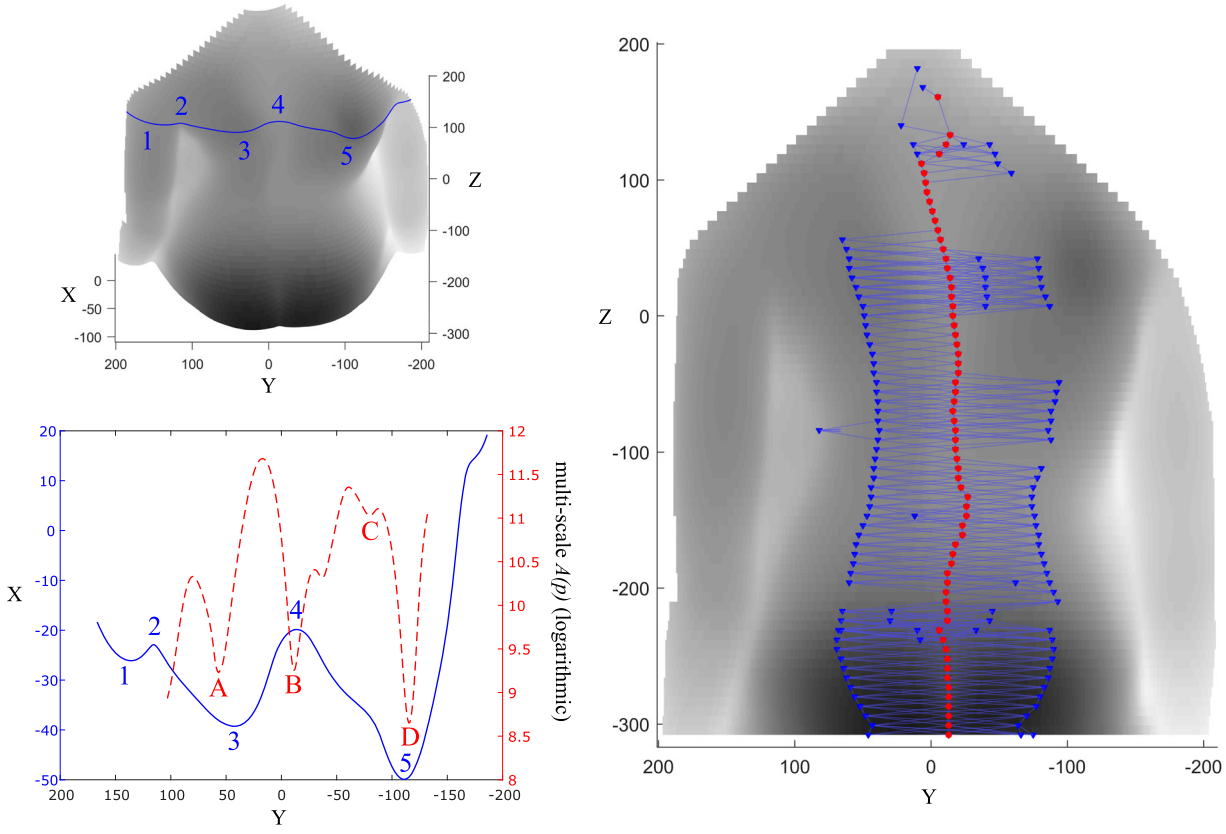


**Figure 4.** An example of the back shape analysis for the *subject 19* (the first experiment). Top left: Interpolated 3D surface with the highlighted transversal slice at $z = 15$. Bottom left: Extracted surface slice at $z = 15$ (full line) and the corresponding values of the *multi-scale* asymmetry map (dashed line). Note multiple local (relative) minima denoted by letters where the absolute minima corresponds to the location of the right scapula. Right: Graph constructed over all relative minima (triangles) with the detected symmetry curve (circles).

To facilitate automatic detection of the symmetry curve, we first filter the asymmetry map in order to reduce a large number of local (relative) minima. Here we propose a *multi-scaling* of the asymmetry function. We compute multiple asymmetry functions using a set of different neighbourhoods $L_i$ and then combine them via multiplication in one final *multi-scale* asymmetry map. Using the a combination over different neighbourhoods (scales) we successfully filter minor symmetries (spurious minima) which are inconsistent over multiple scales.

Next, we propose the *(semi-)automatic* symmetry curve extraction using a novel approach based on the graph theory. The *multi-scale* asymmetry map has many relative minima which correspond to the "true" symmetry curve, and in each profile there may be a few relative minima which should be disregarded. Therefore, we construct a graph structure over the relative minima, and knowing the starting and the ending point of the symmetry curve, we find the shortest path between them which then corresponds to the objective back symmetry curve. The starting and the ending point of the symmetry curve can be detected automatically by finding distinctive anatomical landmarks (C7 and S1/S3 or a midline point between lumbar dimples) [36,37], by placing markers on the patient's back or manually after the 3D acquisition (hence "*semi-*"). The basic algorithm is explained in the text below and described by Algorithm 1.

We first create a directed weighted graph $\mathcal{G}$ defined with set of nodes $\mathcal{V}$, where each node corresponds to one extracted relative minima, and a set of edges $\mathcal{E}$ (*ordered* pairs of nodes). Node pairs representing edges are constructed by connecting nodes using a profile-to-profile principle. Starting from the most cranial profile all the way to the most caudal profile, we connect each minima from one profile with all the minima in the first succeeding profile. All edges between nodes are assigned with weights equal to the Euclidean distance between 3D coordinates (recall that each minima is associated with a point on the previously reconstructed 3D surface).

Rarely, it is possible that Algorithm 1 results in a disconnected graph $\mathcal{G}$. Such result may be induced by holes in the 3D reconstructed surface, by noise in the curvature analysis, or by some other cause that prevents the sequential profile-to-profile approach. We connect the disconnected graph components by adding edges between two nodes from two mutually disconnected components that are nearest by Euclidean distance. Finally, the shortest path $\mathcal{P} = (v_1, v_2, \ldots, v_n)$ between the preknown starting point $(v_1)$ and the ending point

($v_n$) can be found using a standard Dijkstra's algorithm [38]. The 3D coordinates of the points included in the path $\mathcal{P}$ represent the symmetry curve.

**Input:** A set of relative minima $m_k$, $k = 1, ..., N_{rel\_minima}$ with the corresponding 3D coordinates
**Output:** A directed weighted graph $\mathcal{G}$
$S \leftarrow \{\}$; $T \leftarrow \{\}$; $W \leftarrow \{\}$;
**for** $p \leftarrow 2$ **to** $N_{profiles}$ **do**
  $s \leftarrow \{m_k\}, k \in (p-1)$-th profile;
  $t \leftarrow \{m_k\}, k \in p$-th profile;
  **for** $i \leftarrow 1$ **to** $length(s)$ **do**
    **for** $j \leftarrow 1$ **to** $length(t)$ **do**
      $S = \{S\ s_i\}$;
      $T = \{T\ t_j\}$;
      $W = \{W\ dist(s_i, t_j)\}$;
    **end**
  **end**
**end**
$\mathcal{V} = \{m_k\}, k = 1, ..., N_{rel\_minima}$;
$\mathcal{E} = (S, T)$;
$\mathcal{G} = (\mathcal{V}, \mathcal{E}, W)$;

**Algorithm 1:** Basic graph construction to find the symmetry curve.

## 4. Results and discussion

We evaluated the proposed method for the symmetry curve detection in two scenarios. We first assessed the performance of our method by comparing it with the commercial system for functional 3D spine and posture analysis – Diers Formetric [21]. This scanning system is limited to the upright standing (or sitting) positions only and therefore our first experiment included analyses of such postures. The second experiment was designed to test how the proposed method performs when analysing 3D reconstructions in dynamic conditions. In this experiment we investigated the movement most frequently used in physical examinations for spinal deformities – the standing forward bending motion.

### 4.1. Upright standing position

We collected in total 22 back shape recordings using the Diers Formetric system (hereinafter, the Diers method). From the obtained data, for this experiment we used data describing reconstructed surface 3D points and the detected symmetry line (*csl*, central symmetry line). Additionally, we used the detected vertebra prominens (C7) landmark and sacrum landmark as estimates of the vertices $v_1$ and $v_n$. The data include both male and female subjects of different ages and with different severities of deformations.

The 3D surface reconstruction data contain only the 3D coordinates of the surface points. In order to apply our method for the symmetry curve detection on the extracted point cloud, first we computed the 3D surface normals for each point. After that, we applied the proposed symmetry curve detection procedure described in Section 3.3.1.

For the comparison between the Diers method and our method we used a root mean square deviation (RMSD) as a disagreement measure. We interpolated detected curves using splines and compared coordinate values every 1 mm from the highest to the lowest part of the back (where both curves coincides). That gave us in total $N$ points to compare. The lateral deviation of the symmetry curve is the most important feature when assessing scoliotic deformities so we present our results using the RMSD of $y$-coordinates (right-to-left) as a disagreement measure. The RMSD of the $z$-coordinates will be equal to zero as both curves are sampled at the same $z$ coordinates. The $x$-coordinates (back-to-front) are depth values which are dependent on the lateral deviation of the symmetry curve and it is expected that RMSD of $x$-coordinates is negligible compared to the palpation error. If $Y_1$ is a set of $y$-coordinates of the symmetry curve detected using the Diers method, and $Y_2$ is a set of $y$-coordinates of the symmetry curve detected using the proposed method, the $\mathrm{RMSD}_Y$ is computed using:

$$\mathrm{RMSD}_Y = \sqrt{\frac{1}{N}\sum_{i=1}^{N}\left(Y_{1,i} - Y_{2,i}\right)^2}. \qquad (3)$$

The minimal $\mathrm{RMSD}_Y$ was 0.87 mm, the maximal 5.54 mm and the mean $2.67 \pm 1.56$ mm as shown in Figure 5. As expected, $\mathrm{RMSD}_X$ was very low, under one millimetre with the mean equal to $0.67 \pm 0.16$ mm. This experiment showed that the proposed method is comparable with the output of the commercial 3D back surface analysis system within the limits of physicians' palpation error [39–41].

A visual inspection (Figure 6) revealed that some of the higher valued errors may originate from small multiple inflexions of the symmetry curve. This could be eliminated with smart curve smoothing [42] rather than relying on some predefined spine model. Also, the experiment showed that the computation of the surface curvature using method [35] is very dependent on the quality of the surface normal computation which depends on the used spatial neighbourhood around the point, and on the density and the noise in the point cloud. For example, the *subject 13* has a more prominent left scapula and the mean surface curvature of that scapula merged with the curvature of the posterior median furrow and the symmetry curve was detected in the centre of that merged region (as expected from the algorithm).

Another example of the higher RMSD score can be seen in the symmetry curve detection for the *subject 19*. Here we see that the proposed method detected the symmetry curve as valid symmetrical points if we

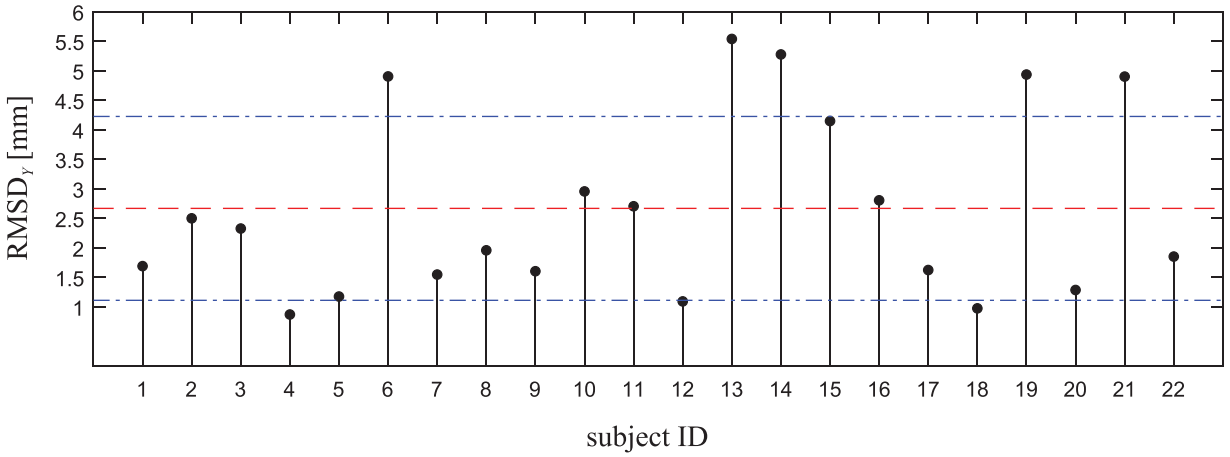


**Figure 5.** RMSD between the Diers method and the proposed method computed for 22 subjects. The dashed line represents the mean value, and the dash-dotted lines one standard deviation.

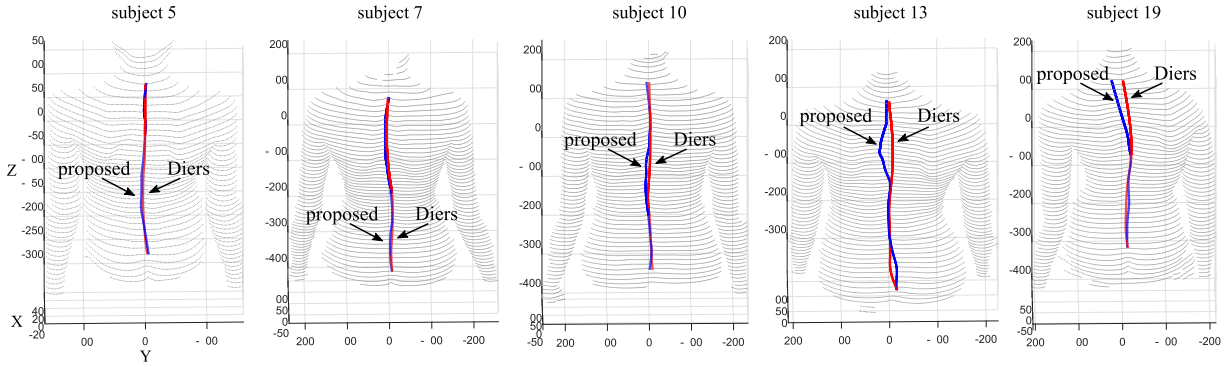


**Figure 6.** Examples of symmetry curve detection for five subjects. The csl curves provided by the Diers method and the symmetry curves obtained using the proposed method are denoted with corresponding arrows.

compare curve's position with the mean surface curvature map of the subject's back (Figure 7). In this case, we have not noticed any "curvature merging" which would cause the symmetry curve to deflect to the left. Therefore, we computed the surface curvature using a third-party software (MeshLab [43]) and compared it to our surface curvature, and noticed that they coincide. In Figure 8, we demonstrate how our symmetry curve better follows the mean surface curvature computed using MeshLab. We assume that the difference between our method and the Diers method may be caused by fitting a curve to a mathematical spine model [20] which is a part of the Diers method. The authors themselves say that "… due to the lack of detailed knowledge of the individual situation, generalized and simplified model assumptions are unavoidable" (p.383 in [20]). This suggests that our result for the *subject 19* is correct and that the result of the Diers method is a generalized solution that may poorly follow an important geometrical property of the surface – its curvature.

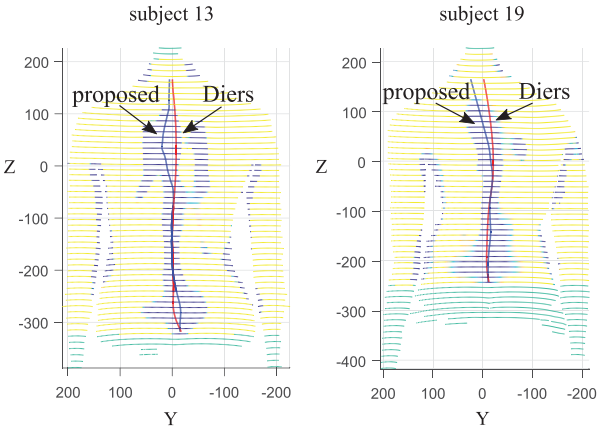


**Figure 7.** Two examples of the higher deviations between the Diers method and the proposed method. On the left we show the incorrect detection of the symmetry curve and on the right the correct detection of the symmetry curve. See text for more details regarding the cause of such behaviour.

### 4.2. Forward bending motion

To show how the proposed method works on postures which are not upright standing positions, we designed the following experiment. Three volunteers were scanned while performing the forward bending motion. They started the motion from the upright standing position and then slowly lowered into the full forward bend position which was still comfortable. This motion is used in diagnostics as a part of the Adam's forward bend test. For each frame captured during

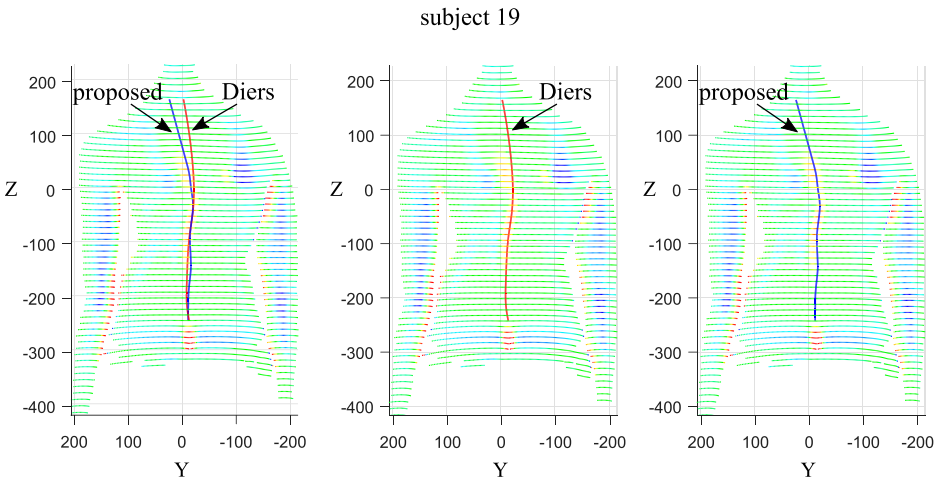


**Figure 8.** Comparison between curves obtained using the Diers method and the proposed method plotted over the point cloud coloured with mean surface curvature values computed using MeshLab. Notice how the proposed method better follows the maximal mean surface curvature region.


**Figure 9.** Input images captured with the dorsal and the ventral scanning unit for frames $f_0$ and $f_{120}$. Notice the black curve drawn on subject's back which was used in the evaluation process.(a) Dorsal scanning unit, frame $f_0$.(b) Dorsal scanning unit, frame $f_{120}$.(c) Ventral scanning unit, frame $f_{120}$.

this motion, we reconstructed the surface of the back using the proposed 3D scanning system as explained in Section 3.2 and applied the proposed method for the symmetry curve detection. The evaluation was done by comparing the detected symmetry curve to the curve which was drawn on subjects' back using a black marker (Figure 9). The hand-drawn black curve was manually annotated and its 3D shape was reconstructed using stereophotogrammetry principle. We utilized the starting and the ending points of the hand-drawn curve as an input for the proposed method for symmetry curve detection as the estimates of the vertices $v_1$ and $v_n$. Instead of that, one could use reflective markers or mark these two points in some other arbitrary manner.

We compared hand-drawn curve with the symmetry curve of the proposed method using the RMSD as a disagreement measure (Equation 3) as in the previous experiment. Each subject completed the forward bending motion within 150 captured frames, and we selected 15 equally spaced frames from that range ($f_0$, $f_{10}, \ldots, f_{130}$, $f_{140}$). The results showed that the detected symmetry curve does not diverge from the hand-marked curve more than the reported physicians' palpation error [39–41]. For the three subjects the average $\text{RMSD}_Y$ was $3.20 \pm 0.78$ , $2.96 \pm 0.45$ and $2.71 \pm 0.64$ mm, respectively (Figure 10).

Figure 11 shows lateral view of the detected 3D symmetry curves (sagittal plane). Each graph illustrates how the symmetry curve changes in time and space during the forward bending motion. The $XY$ plane is parallel with the floor so one can compare how deep the bending was. Also, presenting 3D curves in the sagittal plane can nicely demonstrate how uniform or fast the motion was. This suggest that having a method which can be used to analyse back surface and detect symmetry curves in dynamic motion can be valuable utility for physicians in their back shape analysis.

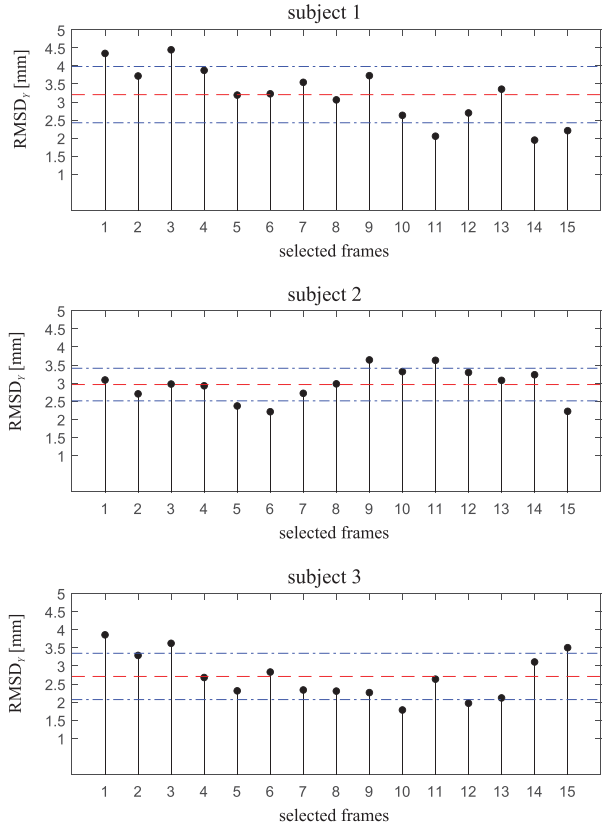


**Figure 10.** RMSD between hand-drawn symmetry curve and the symmetry curve detected using the proposed method computed for tested 15 frames captured during forward bending motion. The dashed line represent the mean value, and dash-dotted line one standard deviation.

## 5. Conclusion

We have proposed a new method for the detection of the back symmetry curve using the 3D reconstruction of the back surface and the analysis of the surface curvatures. The method is based on the multi-scaling of the asymmetry function and (semi-)automatic curve extraction using a novel graph theory-based approach. We have also presented a 3D stereophotogrammetry scanner which can be used to reconstruct the 3D surface of subjects' back while preforming the forward bending motion. We have used the proposed 3D scanner to evaluate the applicability of the proposed method for the symmetry curve detection in time during the forward bending process. We have compared the proposed method with one commercial 3D system and with the manually determined symmetry curve and the results were comparable. The main strength of this paper is the method's ability to detect symmetry curves in both the upright and the forward bend positions while retaining errors in the range of physicians' palpation.

## Note

1. Midline longitudinal depression in the surface of the back; it begins superiorly in the cervical region and is continuous inferiorly with the gluteal cleft, diminishing at the base of the neck and over the sacral base [11].

## Disclosure statement

No potential conflict of interest was reported by the authors.

## Funding

This work was supported by Croatian Science Foundation [grant no. IP-11-2013-3717].

## ORCID

*Matea Đonlić* http://orcid.org/0000-0001-5165-6438
*Tomislav Petković* http://orcid.org/0000-0002-3054-002X

## References

[1] National Scoliosis Foundation. The importance of early detection. [cited 2018 Mar 19]. Available from: http://www.scoliosis.org/early-detection
[2] Weinstein SL, Dolan LA, Cheng JC, et al. Adolescent idiopathic scoliosis. Lancet. 2008;371(9623):1527–1537. doi:10.1016/s0140-6736(08)60658-3

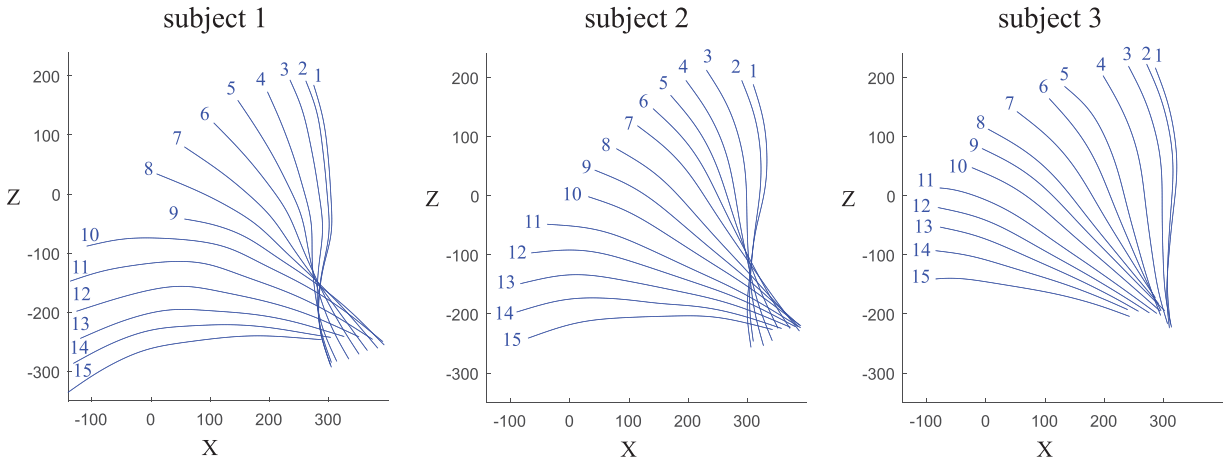


**Figure 11.** Time-lapse showing detected symmetry curves for the three subjects in the sagittal plane. The origin of the coordinate system is the origin of the calibration board which was used to calibrate the 3D scanning system.

[3] Good CR, Auerbach JD, O'Leary PT, et al. Adult spine deformity. Curr Rev Musculoskelet Med. 2011;4(4):159–167. doi:10.1007/s12178-011-9101-z
[4] Physiopedia. Adam's forward bend test; 2018. [cited 2018 Apr 10]. Available from: https://www.physiopedia.com/index.php?title=Adam%27s_forward_bend_test&oldid=196159
[5] Nastavni zavod za javno zdravstvo dr Andrija Štampar. Program specifičnih i preventivnih mjera zdravstvene zaštite učenika osnovnih i srednjih škola. [cited 2017 Mar 19]. Available from: http://www.stampar.hr/hr/program-specificnih-i-preventivnih-mjera-zdravstvene-zastite-ucenika-osnovnih-i-srednjih-skola
[6] National Scoliosis Foundation. Scoliosis screening map. [cited 2018 Mar 19]. Available from: http://www.scoliosis.org/information/map
[7] Pasha S, Cahill PJ, Dormans JP, et al. Characterizing the differences between the 2D and 3D measurements of spine in adolescent idiopathic scoliosis. Eur Spine J. 2016;25(10):3137–3145. doi:10.1007/s00586-016-4582-5
[8] Turner-Smith AR, Harris J, Houghton GR, et al. A method for analysis of back shape in scoliosis. J Biomech. 1988;21(6):497–509. doi:10.1016/0021-9290(88)90242-4
[9] Berryman F, Pynsent P, Fairbank J, et al. A new system for measuring three-dimensional back shape in scoliosis. Eur Spine J. 2008;17(5):663–672. doi:10.1007/s00586-007-0581-x
[10] D'Amico M, Kinel E, Roncoletta P. Normative 3D opto-electronic stereo-photogrammetric posture and spine morphology data in young healthy adult population. PLoS ONE. 2017;12(6):1–31. doi:10.1371/journal.pone.0179619
[11] Farlex Partner Medical Dictionary. Posterior median furrow; 2012. [cited 2018 Mar 29]. Available from: https://medical-dictionary.thefreedictionary.com/posterior+median+furrow.
[12] Cappetti N, Naddeo A. A survey of methods to detect and represent the human symmetry line from 3D scanned human back. Cham: Springer International Publishing; 2017.p. 797–808. doi:10.1007/978-3-319-45781-9_80
[13] Hierholzer E. Analysis of left-right asymmetry of the back shape of scoliotic patients. Coblentz AM, Herron RE, editors. Proc. SPIE; Vol. 602; 1986. p. 266–271. doi:10.1117/12.956324
[14] Poredoš P, Čelan D, Možina J, et al. Determination of the human spine curve based on laser triangulation. BMC Med Imag. 2015;15(2):1–11. doi:10.1186/s12880-015-0044-5
[15] Drerup B. Rasterstereographic measurement of scoliotic deformity. Scoliosis. 2014;9(1):1–14. doi:10.1186/s13013-014-0022-7
[16] Daanen H, Haar FT. 3D whole body scanners revisited. Displays. 2013;34(4):270–275. doi:10.1016/j.displa.2013.08.011
[17] Frobin W, Hierholzer E. Rasterstereography: a photogrammetric method for measurement of body surfaces. Photogram Eng Remote Sens. 1981;47(12):1717–1724. Available from: https://www.asprs.org/wp-content/uploads/pers/1981journal/dec/1981_dec_1717-1724.pdf
[18] Frobin W, Hierholzer E. Analysis of human back shape using surface curvatures. J Biomech. 1982;15(5):379–390. doi:10.1016/0021-9290(82)90059-8
[19] Drerup B, Hierholzer E. Back shape measurement using video rasterstereography and three-dimensional reconstruction of spinal shape. Clin Biomech. 1994;9(1):28–36. doi:10.1016/0268-0033(94)90055-8
[20] Drerup B, Hierholzer E. Assessment of scoliotic deformity from back shape asymmetry using an improved mathematical model. Clin Biomech. 1996;11(7):376–383. doi:10.1016/0268-0033(96)00025-3
[21] DIERS biomedical solutions. [cited 2018 Mar 19]. Available from: http://www.diersmedical.com/
[22] Di Angelo L, Di Stefano P, Vinciguerra GM. Experimental validation of a new method for symmetry line detection. Comput Aided Des Appl. 2011;8(1):71–86. doi:10.3722/cadaps.2011.71-86
[23] Di Angelo L, Di Stefano P, Raimondi P, et al. Validation of a method for symmetry line detection. Proceedings of XX International Conference of Graphic Engineering; 2008 Jun 4–6. Available from: http://www.scoliosiricerca.it/index2.php?option=com_docman&task=doc_view&gid=24&Itemid=3
[24] Kuhnel W. Differential geometry: curves-surfaces-manifolds. 2nd ed. American Mathematical Society; 2002. Chapter Curves in $\mathbb{R}^n$; p. 7–55.
[25] Di Angelo L, Di Stefano P, Spezzaneve A. A method for 3D detection of symmetry line in asymmetric postures. Comput Methods Biomech Biomed Eng. 2012;16(11):1–8. doi:10.1080/10255842.2012.659245
[26] Huysmans T, Moens P, Van Audekercke R. An active shape model for the reconstruction of scoliotic deformities from back shape data. Clin Biomech. 2005;20(8):813–821. doi:10.1016/j.clinbiomech.2004.06.015
[27] Cootes T, Taylor C, Cooper D, et al. Active shape models-their training and application. Comput Vis Image Underst. 1995;61(1):38–59. doi:10.1006/cviu.1995.1004
[28] Bergeron C, Cheriet F, Ronsky J, et al. Prediction of anterior scoliotic spinal curve from trunk surface using support vector regression. Eng Appl Artif Intell. 2005;18(8):973–983. doi:10.1016/j.engappai.2005.03.006
[29] DIERS Formetric Technology. 3D/4D Spine & posture analysis. functionality; 2015. [cited 2018 Mar 19]. Available from: http://pdf.medicalexpo.com/pdf/diers-international/diers-formetric/68222-166882-_4.html
[30] Tippetts B, Lee DJ, Lillywhite K, et al. Review of stereo vision algorithms and their suitability for resource-limited systems. J Real-Time Image Process. 2013;11(1):5–25. doi:10.1007/s11554-012-0313-2
[31] Zhang Y, Xiong Z, Cong P, et al. Robust depth sensing with adaptive structured light illumination. J Vis Commun Image Represent. 2014;25(4):649–658. doi:10.1016/j.jvcir.2013.06.003
[32] Petković T, Pribanić T, Đonlić M, et al. Software synchronization of projector and camera for for structured light 3D body scanning tomislav. Proceedings of the 7th International Conference on 3D Body Scanning Technologies; 2016 Nov 30–Dec 1; Lugano, Switzerland. Nov; Ascona: Hometrica Consulting - Dr. Nicola D'Apuzzo; 2016. p. 286–295. doi:10.15221/16.286
[33] Petković T, Pribanić T, Đonlić M, et al. Multi-projector multi-camera structured light 3D body scanner. Proceedings of 3DBODY.TECH 2017 - 8th International Conference and Exhibition on 3D Body Scanning and Processing Technologies; 2018 Oct 11–12. Montreal QC: Hometrica Consulting - Dr. Nicola D'Apuzzo; 2017. doi:10.15221/17.319

[34] Bronshtein I, Semendyayev K, Musiol G, et al. Handbook of mathematics. 5th ed. Berlin: Springer-Verlag; 2007. Chapter Geometry (Subchapter Curvature of a surface); p. 243–250. doi:10.1007/978-3-540-72122-2

[35] Wilson RC, Hancock ER. Consistent topographic surface labelling. Pattern Recognit. 1999;32(7):1211–1223. doi:10.1016/S0031-3203(98)00146-0

[36] Drerup B, Hierholzer E. Automatic localization of anatomical landmarks on the back surface and construction of a body-fixed coordinate system. J Biomech. 1987;20(10):961–970. doi:10.1016/0021-9290(87)90325-3

[37] Bonnet V, Yamaguchi T, Dupeyron A, et al. Automatic estimate of back anatomical landmarks and 3D spine curve from a Kinect sensor. 6th IEEE International Conference on Biomedical Robotics and Biomechatronics (BioRob); June 26–29; Singapore. Singapore: IEEE; 2016. doi:10.1109/biorob.2016.7523746

[38] Cormen TH, Leiserson CE, Rivest RL, et al. Introduction to Algorithms. 3rd ed. The MIT Press; 2009. Chapter Single-Source Shortest Paths (Subchapter Dijkstra's algorithm); p. 658–664. Available from: https://mitpress.mit.edu/books/introduction-algorithms-third-edition

[39] Hart J, Neely C. Allowing a possible margin of error when assessing student skills in spinous process location. J Chiropr Educ. 2011;25(2):182–185. Available from: https://www.ncbi.nlm.nih.gov/pmc/articles/PMC3204954

[40] Schmid S, Studer D, Hasler CC, et al.. Using skin markers for spinal curvature quantification in main thoracic adolescent idiopathic scoliosis: an explorative radiographic study. PLoS ONE. 2015;10(8):e0135689. doi:10.1371/journal.pone.0135689

[41] Mieritz RM, Kawchuk GN. The accuracy of locating lumbar vertebrae when using palpation versus ultrasonography. J Manipulative Physiol Ther. 2016;39(6):387–392. doi:10.1016/j.jmpt.2016.05.001

[42] Machler MB. Variational solution of penalized likelihood problems and smooth curve estimation. Ann Stat. 1995;23(5):1496–1517. doi:10.1214/aos/1176324309

[43] Cignoni P, Callieri M, Corsini M, et al. MeshLab: an open-source mesh processing tool. Scarano V, Chiara RD, Erra U, editors. Eurographics Italian Chapter Conference. The Eurographics Association; 2008. doi:10.2312/LocalChapterEvents/ItalChap/ItalianChapConf2008/129-136